Prediction of gas volume fraction in fully-developed gas-liquid flow in a vertical pipe

A S M Atiqul Islam[1], N A Adoo[1], D J Bergstrom[1], D F Wang[2]

1) Dept. of Mechanical Engineering, University of Saskatchewan, Saskatoon, Canada
2) Canadian Nuclear Laboratories, Chalk River, Ontario, Canada
(nana.adoo@usask.ca)

Abstract

An Eulerian-Eulerian two-fluid model has been implemented for the prediction of the gas volume fraction profile in turbulent upward gas-liquid flow in a vertical pipe. The two-fluid transport equations are discretized using the finite volume method and a low Reynolds number k-ε turbulence model is used to predict the turbulence field for the liquid phase. The contribution to the effective turbulence by the gas phase is modeled by a bubble induced turbulent viscosity. For the fully-developed flow being considered, the gas volume fraction profile is calculated using the radial momentum balance for the bubble phase. The model potentially includes the effect of bubble size on the interphase forces and turbulence model. The results obtained are in good agreement with experimental data from the literature. The one-dimensional formulation being developed allows for the efficient assessment and further development of both turbulence and two-fluid models for multiphase flow applications in the nuclear industry.

1. Introduction

Multiphase flow is a common phenomenon in many environmental and industrial applications in which one component occurs as droplets, bubbles or particles which are distributed throughout the corresponding continuous phase. Bubble columns are often used in chemical engineering applications, where gas bubbles are driven by buoyancy through a stationary liquid phase. A related phenomenon is bubbly flow in a pipe, where gas bubbles occur within a continuous liquid phase driven by a pressure gradient. Gas-liquid flow in a pipe is of special relevance to the nuclear industry, since boiling heat transfer commonly occurs within reactor systems.

In multiphase flow, the relative motion of the phasic constituents is very significant. For gas-liquid flow in a pipe, the development of the flow pattern primarily depends on the forces acting on the bubbles causing either bubble coalescence or bubble break-up [1]. For a turbulent gas-liquid flow, the turbulence induced in the liquid phase by the dispersed gas bubbles can also be important. In order to analyze gas-liquid pipe flow, it is necessary to identify the flow regime which determines the flow conditions and void patterns in the pipe [2]. Transition among the flow regimes depends on such parameters as: pressure, viscosity, surface tension and pipe diameter [2, 3].

Among the different flow regimes, the bubbly flow regime is frequently encountered in many industrial applications. This paper considers gas-liquid flow in the bubbly flow regime where the size of the bubbles depends on the nature of the gas distribution and the physical properties of the liquid. Brennen [4] indicates that the dominant force resisting break-up of bubbles is due to surface tension, while the dominant force promoting bubble break-up is due to shear in the flow. Within this regime, both experimental and theoretical studies have investigated the distribution of bubbles across the pipe diameter, which is characterized by the volume fraction or hold-up profile. More recently, computational fluid dynamics (CFD) has also been applied to multiphase flow in order to develop predictive models for the flow properties, including the volume fraction.

Lucas *et al.* [1] experimentally measured the cross-sectional distribution of the gas volume fraction and bubble size distributions in a vertical pipe for air-water bubbly and slug flow regimes using a high resolution wire-mesh sensor probe. The data obtained is especially useful for the development of numerical models which account for the various forces acting on a bubble, as well as bubble coalescence and break-up. Prasser *et al.* [5] experimentally investigated the evolution of gas–liquid flow structure in a large vertical pipe using a high resolution wire-mesh sensor for the bubbly, slug and churn turbulent flow regimes. They also studied the influence of the physical properties of the fluid by comparing results for experiments of air-water and steam-water mixtures.

Gas-liquid pipe flow can be modeled using a two-fluid formulation. In addition to the drag forces which dominate the momentum exchange in the flow direction, the non-drag forces acting perpendicular to the flow direction play an important role for the development of the hydrodynamic flow structure [6]. So called one-dimensional flows, which correspond to the case of fully developed pipe flow, are especially appealing as a simplified flow paradigm which characterizes the flow in relatively long pipe sections. The fact that the axial gradients of the flow variables are negligible substantially simplifies the set of transport equations to be solved, while still preserving the most essential flow physics. By assuming a generic form for the volume fraction profile and using a drift-flux model, Vitankar and Joshi [7] implemented a stepwise iterative procedure for predicting the gas volume fraction and axial component of the liquid phase mean velocity for bubble columns using a low Reynolds number k-ε model. This one-dimensional CFD model was also extended for the prediction of pressure drop for two-phase gas-liquid flow in bubble columns. In spite of the large number of one-dimensional models documented in the literature since 1980, such issues as: appropriate closure for turbulent and multiphase models, proper description of interface momentum and energy transfer, modelling of radial movement of bubbles, and the overall energy and mass balance still remain challenging issues for one-dimensional model formulations [7]. Ekambara [8] carried out CFD simulations for predicting the flow pattern in cylindrical bubble column reactors for one, two and three-dimensional flows using a k-ε turbulence model, and observed good agreement with experimental measurements for the axial liquid velocity and fractional gas volume fraction profiles, especially for the three-dimensional model predictions.

One of the challenging aspects of gas-liquid flow analysis for fully developed pipe flow is prediction of the radial gas volume fraction profile, since the continuity equations are identically satisfied by the fully-developed flow assumption. In such cases, Lucas *et al.* [9] have shown that the volume fraction distribution is governed by the radial force balance on the bubbles. The present paper documents a numerical study of turbulent fully-developed bubbly liquid-gas flow in a vertical pipe using the approach of Lucas *et al.* [9]. The turbulent liquid-phase turbulence is solved from the low Reynolds number k-ε model of Myong and Kasagi [10], where the source terms of Dhotre *et al.* [11] have been implemented to represent the effect of the bubble phase on the turbulence. Results are presented for the case of a flow pattern characterized by a centre peak value for the gas volume fraction profile. One advantage of studying this one-dimensional flow is that it allows the effects of the individual models, both turbulent and multiphase, to be readily evaluated against benchmark data, which is not possible for most complex three-dimensional flows.

2. Computational Method

2.1 Two-fluid model

The governing Reynolds-Averaged Navier–Stokes (RANS) equations for the mean velocity fields are obtained by averaging the conservation of mass and momentum equations for each phase, resulting in a so called Eulerian-Eulerian formulation. The two-fluid model treats both the gas and liquid phases as interpenetrating continua, and uses the local volume fraction of each component to characterize the spatial distribution of the two phases. Coupling between the two phases is achieved through the pressure and interfacial transfer terms in the momentum equations.

2.2 Mathematical formulation

The steady one-dimensional phasic momentum equations for the mean axial velocity components in upward fully developed pipe flow are given below using a cylindrical coordinate system aligned in the flow direction:

$$0 = -\alpha_l \frac{\partial P}{\partial z} + \alpha_l \frac{1}{r}\frac{\partial}{\partial r}\left(r\left(\mu_{eff} \frac{\partial u_z}{\partial r} \right)\right) + \alpha_l \rho_l g - F^D \quad \text{(1a)}$$

$$0 = -\alpha_g \frac{\partial P}{\partial z} + \alpha_g \frac{1}{r}\frac{\partial}{\partial r}\left(r\left(\mu_g \frac{\partial v_z}{\partial r} \right)\right) + \alpha_g \rho_g g + F^D \quad \text{(1b)}$$

In the equations above, the terms on the right hand side represent, respectively, the pressure gradient, effective stress or diffusive transport, gravitational force and interphase momentum exchange terms. Note that the total acceleration for each phase is zero. For the liquid phase, the Reynolds shear stress term is modelled by an eddy viscosity model relation, so that it can be included as the turbulent contribution to the effective stress term. The model parameters along with the constitutive relations used to solve equations (1a) and (1b) are given in *Table 1*. In the current study, only the drag force appears in the interphase momentum exchange term in the streamwise momentum equations, while the other forces acting in the radial direction are used to determine the local gas volume fraction (as described below.)

Table 1 Constitutive relations for the phasic axial momentum equations

Effective viscosity, $\mu_{eff} = \mu_l + \mu_t + \mu_{BIT}$
Volume fraction, $\alpha_g + \alpha_l = 1$
Bubble induced turbulent viscosity [12], $\mu_{BIT} = C_{\mu,BIT}\alpha_g \rho_l d_b \left\| v_z - u_z \right\|$ where $C_{\mu,BIT} = 0.6$
Drag force [13], $F^D = \frac{3}{4}\alpha_g \alpha_l \rho_l \frac{C_D(\mathrm{Re_b})}{d_b}\left\| v_z - u_z \right\|(v_z - u_z)$, $\mathrm{Re_b} = \frac{\rho_l \left\| v_z - u_z \right\| d_b}{\mu_l}$,
where $C_D(\mathrm{Re_b}) = C_\infty + \frac{24}{\mathrm{Re_b}} + \frac{6}{1+\sqrt{\mathrm{Re_b}}}$, $C_\infty = 0.5$

The liquid phase turbulence was modelled by a two-equation *k-ε* model closure. In order to resolve the turbulent flow all the way to the wall and avoid the use of wall functions, the low Reynolds number *k-ε* turbulence model of Myong and Kasagi [10] was implemented. The effect of the bubbles on the turbulence was modelled by the source terms developed by Dhotre *et al.* [11]. The fully developed form of the transport equations for *k* and *ε* is given by the following equations:

$$0 = \frac{1}{r}\frac{\partial}{\partial r}\left(r\alpha_l \left(\mu_l + \frac{\mu_t}{\sigma_k} \right) \frac{\partial k}{\partial r} \right) + \alpha_l \mu_t \left(\frac{\partial u_z}{\partial r} \right)^2 - \alpha_l \rho_l \varepsilon + C_{k1} C_f \alpha_g \alpha_l \rho_l k \tag{2a}$$

$$0 = \frac{1}{r}\frac{\partial}{\partial r}\left(r\alpha_l \left(\mu_l + \frac{\mu_t}{\sigma_\varepsilon} \right) \frac{\partial \varepsilon}{\partial r} \right) + C_1 f_1 \alpha_l \frac{\varepsilon}{k} \mu_t \left(\frac{\partial u_z}{\partial r} \right)^2 - C_2 f_2 \alpha_l \rho_l \frac{\varepsilon^2}{k} + C_{k2} C_f \alpha_g \alpha_l \rho_l \varepsilon \tag{2b}$$

The turbulence model expressions used in these equations are given in *Table 2*.

Table 2 Model relations for the low Reynolds number *k-ε* turbulence model

Turbulent viscosity, $\mu_t = \dfrac{C_\mu f_\mu \rho_l k^2}{\varepsilon}$	$f_1 = 1$
$f_2 = \left(1 - \frac{2}{9}\exp\left(-\frac{R_T}{6}\right)^2\right)\left(1 - \exp\left(-\frac{y^+}{5}\right)\right)^2$,	$f_\mu = \left(1 - \exp\left(-\frac{y^+}{70}\right)\right)\left(1 + \frac{3.45}{\sqrt{R_T}}\right)$
$y^+ = \dfrac{\rho_l u_{wall}(R-r)}{\mu_l}$,	$R_T = \dfrac{\rho_l k^2}{\mu_l \varepsilon}$
$C_f = \frac{3}{4}\left(\frac{C_D}{d_b}\right)\left(\lvert v_z - u_z \rvert\right)$	

Model constants:

$C_1 = 1.40$ $\quad C_2 = 1.80$ $\quad C_\mu = 0.09$ $\quad C_{k1} = 0.15$ $\quad C_{k2} = 0.20$ $\quad \sigma_k = 1.40$ $\quad \sigma_\varepsilon = 1.30$

2.3 Volume fraction prediction

According to Tomiyama [14] the transverse lift force acting on the bubble causes coalescence of the smaller bubbles near the wall for bubble sizes above the critical bubble diameter of 5.8 mm; these in turn drift towards the centre of the pipe due to the wall force. For vertical upward pipe flow, smaller bubbles tend to move towards the wall, while larger bubbles accumulate at the centre [1]. These cases represent *wall-peak* and *centre-peak* gas volume fraction profiles, respectively.

For the bubbly flow regime, the local gas volume fraction is determined based on the radial force balance on the gas bubbles. The lateral forces, which include the lift force, turbulent dispersion force, and wall lubrication force, determine the radial profile of the gas volume fraction [6].

Lucas *et al.* [9] used the following radial force balance to predict the local gas volume fraction, α_g:

$$F^L + F^W + F^{TD} + F^{TD,Eo} = 0 \tag{3}$$

where the lift force, wall lubrication force and turbulent dispersion force correlations are given in *Table 3*.

Table 3 Constitutive relations for the radial force balance

Lift force [9], $F^L = -C_L \alpha_g \rho_l \left(v_z - u_z\right) \dfrac{\partial u_z}{\partial r}$

Wall force [9], $F^W = -C_W \rho_l \left(\dfrac{d_b}{2}\right) \left(v_z - u_z\right)^2 \left(\dfrac{1}{\left(R-r\right)^2} - \dfrac{1}{\left(R+r\right)^2}\right) \alpha_g$

Turbulent dispersion force [9], $F^{TD} = -C_{TD} \rho_l k \dfrac{\partial \alpha_g}{\partial r}$, where $C_{TD} = 0.10$

Turbulent dispersion force based on Eotvos number [9], $F^{TD,Eo} = -C_{D,Eo} \rho_l \left(Eo - 1\right) \dfrac{\partial \alpha_g}{\partial r}$,

where $C_{D,Eo} = 0.0015$

The Tomiyama [14] lift force coefficient

$$C_L = \begin{cases} \min[0.288 \tanh(0.121 \mathrm{Re}_b),\ f(Eo_d)], & Eo_d < 4 \\ f(Eo_d) = 0.00105 Eo_d^3 - 0.0159 Eo_d^3 - 0.0204 Eo_d + 0.474, & 4 \le Eo_d \le 10.7 \\ -0.29, & Eo_d > 10.7 \end{cases}$$

where E_{od} is the Eotvos number based on the long axis d_H of a deformable bubble, and

$$Eo_d = \frac{(\rho_l - \rho_g)\, g\, d_H^2}{\sigma}, \quad d_H = d_b (1 + 0.163 Eo^{0.757})^{1/3}, \quad Eo = \frac{(\rho_l - \rho_g)\, g\, d_b^2}{\sigma}$$

The Tomiyama [14] wall force coefficient

$$C_W = \begin{cases} \exp(-0.933 Eo + 0.179) & if\ \ 1 \le Eo \le 5 \\ \min(0.0059905 Eo - 0.0186865,\ 0.179) & if\ \ Eo > 5 \end{cases}$$

Substituting the various model relations from *Table 3* into equation (3) and rearranging gives the following first-order differential relation for the gas volume fraction:

$$\begin{aligned} &\left(0.1k + C_{D,\mathrm{Eo}} \left(Eo - 1\right)\right) \frac{\partial \alpha_g}{\partial r} \\ &+ \left(C_L \left(v_z - u_z\right) \frac{\partial u_z}{\partial r} + C_W \left(\frac{d_b}{2}\right) \left(v_z - u_z\right)^2 \left(\frac{1}{\left(R-r\right)^2} - \frac{1}{\left(R+r\right)^2}\right)\right) \alpha_g = 0 \end{aligned} \tag{4}$$

2.4 Numerical method

The set of governing equations for the gas-liquid flow given above was discretized using a cell centered implicit finite volume method developed by Patankar [15], and the coupled set of discrete equations was solved using a tri-diagonal matrix algorithm with appropriate boundary conditions. A non-uniform grid consisting of 80 control volumes was used for the simulation with a y^+ value of approximately 0.80 for the first interior control volume.

2.5 Boundary conditions

As summarised in *Table 4*, no-slip boundary conditions were used at the wall and symmetry boundary conditions were applied at the centreline of the pipe.

Table 4 Boundary conditions

At the centre:	$\frac{\partial u_z}{\partial r}=0$	$\frac{\partial v_z}{\partial r}=0$	$\frac{\partial k}{\partial r}=0$	$\frac{\partial \varepsilon}{\partial r}=0$
At the wall:	$u_z=v_z=0$	$k=0$	$\varepsilon=\nu\left(\frac{\partial^2 k}{\partial r^2}\right)$	

3. Results and Discussion

3.1 Flow Conditions

This simulation was performed for the experimental flow conditions (see *Table 5*) considered by Lucas *et al.* [1]. From the experimental data, the average volume fraction was calculated to be $\bar{\alpha}_g=0.20$, and the average (or bulk) liquid velocity was calculated to be $\bar{u}=1.27$ m/s, giving a bulk Reynolds number of Re = 65,000 for the liquid phase. In the simulation, the axial pressure gradient was adjusted to obtain the same value for the bulk Reynolds number for the liquid phase as in the experiment.

Table 5 Flow parameters

Parameters	**Experimental [1]**
Superficial liquid velocity, [m/s]	1.017
Superficial gas velocity, [m/s]	0.219
Pipe diameter (D), [m]	0.0512
Bubble (mean) diameter (d_b), [m]	0.006

3.2 Numerical Results

The numerical model was used to predict the phasic velocity and gas volume fraction profiles for the case of turbulent fully developed upward flow of air and water in a pipe. The simulation results were compared to the measurements of Lucas *et al.* [1], as well as the numerical prediction of Lucas *et al.* [9].

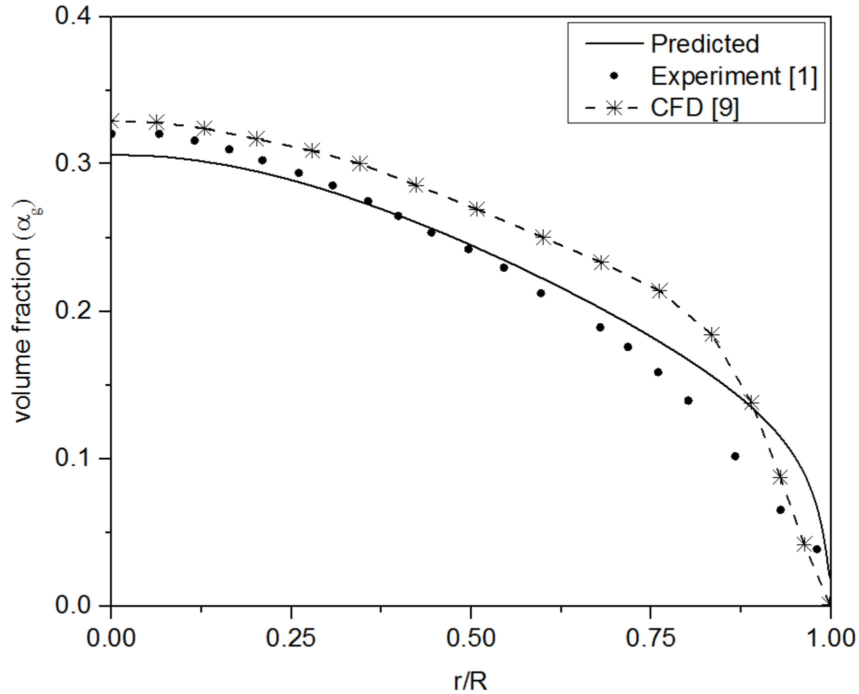

Figure 1 Comparison of gas volume fraction profiles from current prediction and other experimental and numerical studies.

From Figure 1, the predicted gas volume fraction is close to the experimental measurements of Lucas *et al.* [1] and performs somewhat better than the numerical result of Lucas *et al.* [9]. Compared to the experimental data, the current model slightly under- and over-predicts the gas volume fraction near the centre-line and pipe wall, respectively. Note that for this bubble size, the gas volume fraction peaks at the centre of the pipe, which can be attributed to the process whereby smaller bubbles detach from the wall, coalesce into larger bubbles and drift towards the centre of the pipe. The values of the coefficients in the interphase source terms in the k and ε equations were modified from the values used by Dhotre *et al.* [11] to improve the agreement between the predicted and experimental gas volume fraction profiles. Other simulations (not shown) for different bulk gas volume fractions but with the same bubble diameter also predicted similar centre-peak profiles.

Figure 2 presents the predictions for the phasic velocity profiles. From Figure 2, it can be seen that the mean velocity predicted for the liquid phase is in good agreement with the experimental data of Lucas *et al.* [1], although the model slightly over-predicts the experimental values away from the wall. The two-fluid model predicted a superficial gas velocity of 0.254 m/s, whereas the experimental measurement was 0.219 m/s. As such, the model over-predicted the value of the superficial gas velocity by approximately 16%. The slip velocity was observed to be a maximum at the centre-line and decreased towards the wall, as would be expected.

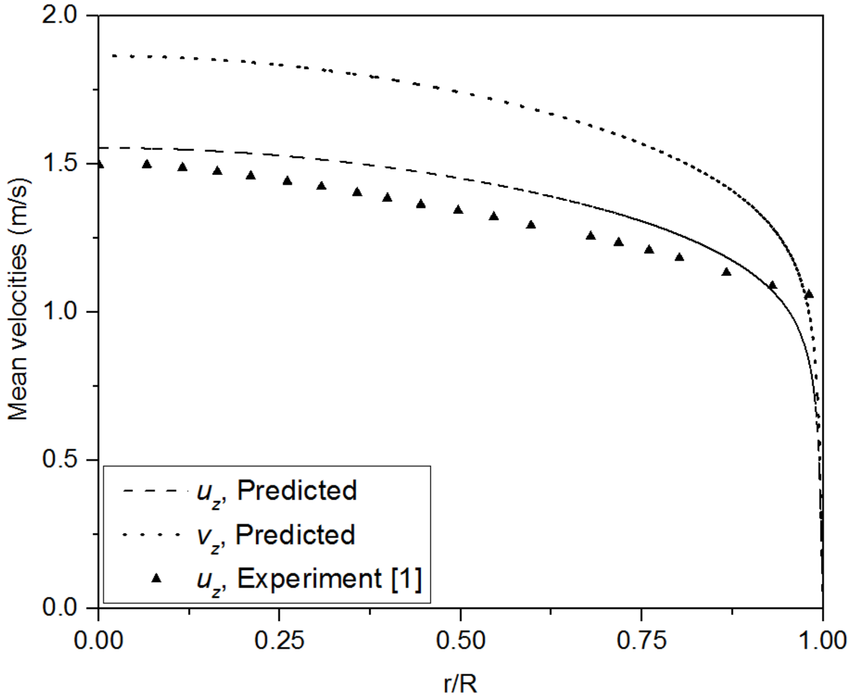

Figure 2 Comparison of liquid (u_z) and gas (v_z) mean velocity profiles with experimental results of Lucas *et al.* [1].

Figure 3 presents the profile for the dimensionless turbulence kinetic energy (k^+) as a function of dimensionless wall normal distance (y^+) for simulations with and without use of a source term in the k and ε equations. The profile for single phase flow was also included for comparison. It turns out that the profile for the turbulence kinetic energy calculated without the source term is almost the same as that for the single phase flow, with only a small difference near the wall. All profiles reproduce the sharp near-wall peak, which is characteristic of near-wall turbulent flow.

In general, the effect of the gas phase is to enhance the level of the turbulence kinetic energy, especially near the centre of the pipe where the gas volume fraction is the highest. The predicted results using modified values for the coefficients, i.e., C_{k1} = 0.15 and C_{k2} = 0.20, for the source terms in the k and ε equations, respectively, showed a much more modest increase in the level of the turbulence kinetic energy due to the bubbles than the results obtained using the values for the model coefficients (C_{k1} = 0.75 and C_{k2} = 0.60) recommended by Dhotre *et al.* [11]. It appears that the source term coefficients used by Dhotre *et al.* [11] are not universal and may depend on the bubble diameter; this issue warrants further investigation as noted by Sheng and Irons [16].

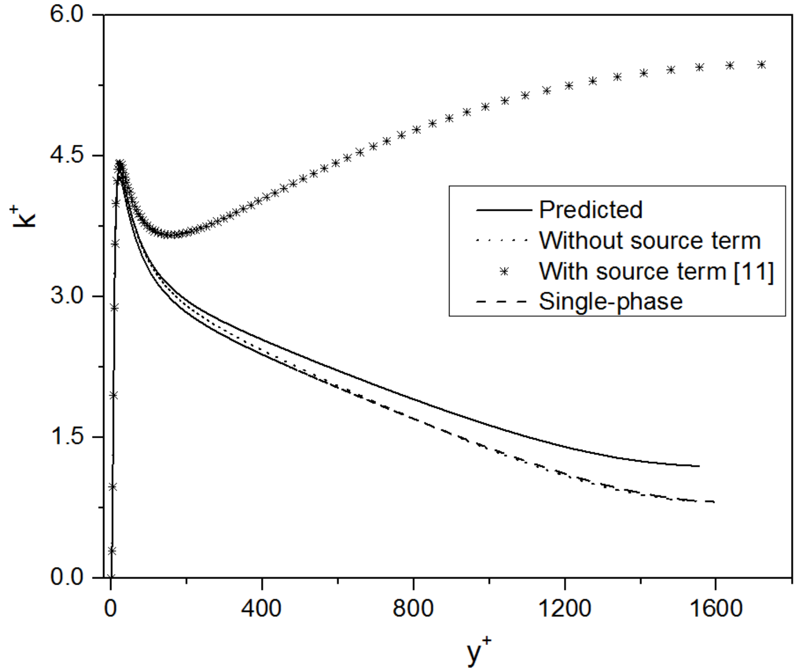

Figure 3 Comparison of dimensionless turbulence kinetic energy profiles for liquid in gas-liquid and single-phase flow, with and without the multiphase source terms.

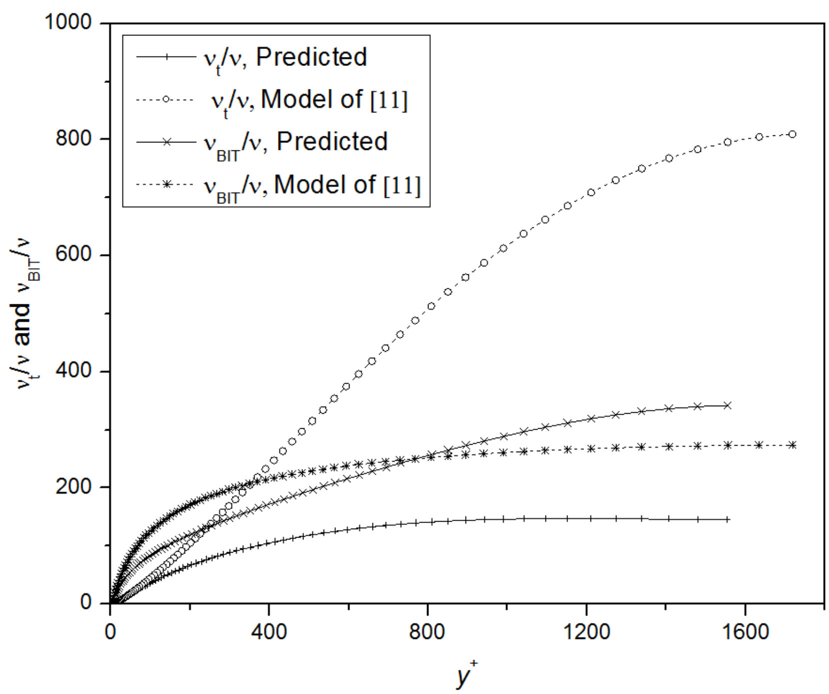

Figure 4 Comparison of eddy and bubble-induced turbulent viscosity profiles for liquid phase.

As shown in Figure 4, the profiles for the conventional eddy viscosity and bubble induced turbulence components of the effective viscosity indicate that for the models and flow conditions used in this study both are approximately the same order of magnitude. For this flow, the turbulent eddy viscosity is relatively small and less than the turbulence generated by the bubbles, which explains why some studies have neglected including a separate turbulence model [13]. Note that in the present two-fluid model formulation, the turbulence kinetic energy was also used to determine the turbulent dispersion force (see Table 3). The viscosity due to the bubble induced turbulence was largest near the centre of the pipe where the gas volume fraction is a maximum.

4. Conclusion

A one-dimensional two-fluid model has been implemented for the prediction of the gas volume fraction, mean phasic velocities and turbulence properties of the liquid phase in fully developed gas-liquid upward flow in a vertical pipe. The gas volume fraction profile was calculated using the radial momentum balance for the bubble phase. The model was able to successfully predict the case of bubbly flow with a centre peak in the volume fraction profile. Modifying the interphase source term coefficients in the k and ε equations resulted in an improved prediction for the gas volume fraction profile and a more realistic profile for the turbulence kinetic energy. For this flow, the bubble induced turbulence was higher compared to the shear-driven turbulence in the liquid phase. The one-dimensional model will facilitate the efficient assessment and further development of both the turbulence and two-fluid model relations for multiphase flow applications in the nuclear industry.

5. Acknowledgements

The authors are grateful to Canadian Nuclear Laboratories (formerly Atomic Energy Canada Limited) for providing financial assistance for this research project.

6. Nomenclature

C_D	Drag coefficient
C_L	Lift coefficient (transverse)
C_W	Wall (lubrication) force coefficient
C_{TD}	Turbulent dispersion force coefficient
$C_{D,Eo}$	Turbulent dispersion force coefficient based on modified Eotvos number
d_b	Gas bubble diameter (mean)
d_H	Long axis bubble diameter
D	Pipe diameter
E_o	Eotvos Number
F^D	Drag force
F^L	Lift force
F^W	Wall (lubrication) force
F^{TD}	Turbulent dispersion force
$F^{TD,Eo}$	Turbulent dispersion force based on a modified Eotvos number
k	Turbulence kinetic energy
P	Pressure
r	Radial variable
R	Pipe radius
Re	Reynolds number (flow)
Re_b	Bubble Reynolds number
u_z	Liquid phase velocity (mean)
v_z	Gas phase velocity (mean)
g	Gravitational acceleration

Greek Symbols

α_g	Gas volume fraction
α_l	Liquid volume fraction
ε	Dissipation of turbulence kinetic energy
ρ_g	Density of gas phase
ρ_l	Density of liquid phase
σ	Surface tension of liquid phase
μ_{eff}	Effective viscosity of liquid phase
μ_g	Dynamic viscosity of gas phase
μ_l	Dynamic viscosity of liquid phase
μ_{BIT}	Bubble induced turbulent viscosity
μ_t	Turbulent viscosity of liquid phase
υ	Kinematic viscosity

Subscripts

b	Bubble
g	Gas phase
l	Liquid phase

7. References

[1] D. Lucas, E. Krepper and H.-M. Prasser, "Development of co-current air–water flow in a vertical pipe", International Journal of Multiphase Flow, Vol. 31, 2005, pp.1304–1328.

[2] A. Shaikh and M. H. Al-Dahhan, "A Review on flow regime transition in bubble columns", International Journal of Chemical Reactor Engineering, Vol. 5, Review R1, 2007.

[3] M. C. Ruzicka, J. Drahos, M. Fialova and N. H. Thomas, "Effect of bubble column dimensions on flow regime transition", Chemical Engineering Science, Vol. 56, 2001, pp.6117-6124.

[4] E. Brennen, "Fundamentals of Multiphase Flow", Cambridge University Press, New York, USA, 2005.

[5] H.-M. Prasser, M. Beyer, H. Carl, S. Gregor, D. Lucas, H. Pietruske, P. Schutz, F.-P. Weiss, "Evolution of the structure of a gas–liquid two-phase flow in a large vertical pipe", Nuclear Engineering and Design, Vol. 237, 2007, pp.1848–1861.

[6] E. Krepper, D. Lucas and H.-M. Prasser, "On the modelling of bubbly flow in vertical pipes", Nuclear Engineering and Design, Vol. 235, 2005, pp.597–611.

[7] V.S. Vitankar, M.T. Dhotre and J.B. Joshi, "A low Reynolds number k–ε model for the prediction of flow pattern and pressure drop in bubble column reactors", Chemical Engineering Science, Vol. 57, 2002, pp.3235–3250.

[8] K. Ekambara, M. T. Dhotre, J. B. Joshi and B. Jyeshtharaj, "CFD simulations of bubble column reactors: 1D, 2D and 3D approach", Chemical Engineering Science, Vol. 60, 2005, pp.6733-6746.

[9] D. Lucas, E. Krepper and H.-M. Prasser, "Prediction of radial gas profiles in vertical pipe flow on the basis of bubble size distribution", International Journal of Thermal Science, Vol. 40, 2001, pp.217–225.

[10] H. K. Myong and N. Kasagi, "A new approach to the improvement of turbulence model for wall-bounded shear flows", JSME Int. J. (II), Vol. 33, Iss. 1, 1990, pp.63–72.

[11] M.T. Dhotre, B.L. Smith and B. Niceno, "CFD simulation of bubbly flows: random dispersion model", Chemical Engineering Science, Vol. 62, 2007, pp.7140–7150.

[12] Y. Sato and K. Sekoguchi, "Liquid velocity distribution in two-phase bubble flow", Int. J. of Multiphase Flow, Vol. 2, Iss. 1, 1975, pp.79–95.

[13] S. M. Monahan and R. O. Fox, "Validation of two-fluid simulations of a pseudo-two dimensional bubble column with uniform and nonuniform aeration", Industrial and Engineering Chemistry Research, Vol. 48, 2009, pp.8134–8147.

[14] A. Tomiyama, "Struggle with computational bubble dynamics", Third International Conference on Multiphase Flow, Lyon, France, 1998 June 8–12.

[15] S.V. Patankar, "Numerical Heat transfer and Fluid Flow", Hemisphere, New York, 1980

[16] Y.Y. Sheng and G.A. Irons, "Measurement and modeling of turbulence in the gas liquid two-phase zone during gas injection", Metallurgical Transactions B 24, 1993, pp. 695–705.